Electron states scattering off line edges on the surface of topological insulator*

Shao Huai-Hua(邵怀华), Liu Yi-Man(刘一曼), Zhou Xiao-Ying(周小英), and Zhou Guang-Hui(周光辉)†

Department of Physics and Key Laboratory for Low-Dimensional Structures and Quantum Manipulation (Ministry of Education), Hunan Normal University, Changsha 410081, *China*

(Received 25 April 2014; revised manuscript received 20 May 2014; published online 10 August 2014)

We study the local density of states (LDOS) for electrons scattering off the line edge of an atomic step defect on the surface of a three-dimensional (3D) topological insulator (TI) and the line edge of a finite 3D TI, where the front surface and side surface meet with different Fermi velocities, respectively. By using a δ-function potential to model the edges, we find that the bound states existed along the step line edge significantly contribute to the LDOS near the edge, but do not modify the exponential behavior away from it. In addition, the power-law decaying behavior for LDOS oscillation away from the step is understood from the spin rotation for surface states scattering off the step defect with magnitude depending on the strength of the potential. Furthermore, the electron refraction and total reflection analogous to optics occurred at the line edge where two surfaces meet with different Fermi velocities, which leads to the LDOS decaying behavior in the greater Fermi velocity side similar to that for a step line edge. However, in the smaller velocity side the LDOS shows a different decaying behavior as $x^{-1/2}$, and the wavevector of LDOS oscillation is no longer equal to the diameter of the constant energy contour of surface band, but is sensitively dependent on the ratio of the two Fermi velocities. These effects may be verified by STM measurement with high precision.

Keywords: topological insulator, line defects, local density of states

PACS: 73.50.–h, 72.80.Vp, 73.23.–b **DOI:** 10.1088/1674-1056/23/10/107304

1. Introduction

Topological insulators (TIs),[1,2] which are a recently discovered new phase of quantum matter, have been extensively studied theoretically[3–6] and experimentally[7–11] due to the distinct surface states and potential relevance for spintronic applications.[12,13] The three-dimensional (3D) TIs are characterized by the gapped bulk and gapless surface states, which are protected by the time-reversal symmetry (TRS).[6] In a 3D TI, the electron has strong spin–orbit coupling, and the surface states are described by a low-energy effective massless Dirac equation in which the spin orientation is determined by its momentum vector.[6] Several important features of these Dirac surface states on the surface of a 3D TI, such as Majorana fermions,[14,15] magnetic monopole,[15] quantum phase transitions,[17–19] magnetic proximity effects,[20] electron–electron interactions,[21] and spin polarization,[22] and charge transmission[23] in confined states, etc., have been investigated.

Scanning tunneling microscopy (STM) provides a direct way to study surface states, which is highly relevant for future attempts to design nanoelectronic and spintronic devices based on these materials, through probing the local density of states (LDOS) in the vicinity of impurities or defects. Experiments on STM and theories describing the quasiparticle interference patterns induced by nonmagnetic point impurities[24–28] or atomic step line edges[29–40] on 3D TI surfaces and nanofilms, have recently been formulated. The LDOS oscillations away from a step edge on both surfaces of Bi_2Se_3 with nearly isotropic Dirac cone and Bi_2Te_3 with strongly warped surface band, show a power-law decay $x^{-3/2}$ in the low energy case,[35] with x being the distance from the step edge. This faster decay, in contrast with the $x^{-1/2}$ decay seen in a conventional two-dimensional electron gas (2DEG),[41] is believed to result from the suppression of backscattering on surface of a 3D TI, where the wave vector of LDOS oscillation is equal to the diameter of the constant-energy contour (CEC). This has been used to confirm the linear dispersion and infer the Fermi velocity on the Dirac cone in Bi_2Te_3 crystal.[24] However, the LDOS behavior very near a step edge on the surface strong 3D TI observed experimentally is not well explained. On the other hand, a finite strong 3D TI may have front and side surfaces with (111) and (221) in Miller indices of the rhombohedral bulk structure, respectively. A number of works[42–44] have predicted that there exist chiral side surface states and refractive transport across the line edge where the two surfaces meet with different Fermi velocities. However, the LDOS near the edge line has not yet been considered. This is also important for a further understanding the nature of 3D TI surfaces.

In this work, by adding a δ-function model potential to the effective low-energy surface Hamiltonian for a 3D TI, we

*Project supported by the National Natural Science Foundation of China (Grant No. 11274108), the Specialized Research Fund for the Doctoral Program of Higher Education of China (Grant No. 20114306110008), and the Hunan Provincial Innovation Foundation for Postgraduates (Grant No. CX2012B204).

†Corresponding author. E-mail: ghzhou@hunnu.edu.cn

© 2014 Chinese Physical Society and IOP Publishing Ltd

study the decaying behavior of LDOS oscillations both near and away from an atomic step line edge on a single surface of a semi-infinite strong 3D TI and a line edge of a finite 3D TI where two surfaces meet with different Fermi velocities, respectively. Firstly, for the step line edge on a single TI surface, we find that the bound states existed along the step edge[33,40,45] significantly contribute to the LDOS in the vicinity of the step defect. However, this contribution of bound states has not been taken into account for LDOS because it does not modify the decay exponent of the LDOS oscillating behavior away from the step edge. In addition, the spin rotation for surface states across the step edge,[36] with the magnitudes depending on the strength of the δ-function potential. Secondly, for a line edge, the electron refraction and total reflection phenomenons analogous to optics occur across the edge where the two surfaces meet with different Fermi velocities.[42] This has been also studied at the junction between the surfaces of two TIs in Ref. [44]. Our work is mainly concerned with the distributions of LDOS near the line edges. Especially, we get a new decaying behavior at corner boundary of a topological insulator. By ignoring the influence of the bound states, we find that the LDOS oscillating decay behavior in the greater Fermi velocity side is similar to that for a step line edge on a single TI surface. While in the smaller Fermi velocity side, the LDOS oscillations near the line edge show a slower decay as $x^{-1/2}$, which is in contrast with the $x^{-3/2}$ decay seen for the step line edge. In this case the wavevector of the LDOS oscillation is no longer equal to the diameter of the CEC of surface band, but it is sensitively dependent on the ratio of the two Fermi velocities.

The organization of this paper is as follows. In Section 2, we formulate the model Hamiltonian for a step line edge on the surface of a 3D TI, and show that the bound states make an important contribution to the total LDOS in the vicinity of the step edge on the surface. We present the LDOS oscillations decaying behavior induced by a line edge where surfaces with different Fermi velocities meet and discuss the result, which is different from that for a line step edge in Section 3. And in Section 4, we draw a summary.

2. A step line defect on the single surface of an infinitive 3D TI

The atomic structure defects are actually unavoidable in real TI samples. Here, we model an atomic step on the surface of a 3D TI as a δ-function scattering potential rather than a step-function potential because there is no potential difference across the step edge, as pointed out by An and Ting.[37,38] For the step-function potential, a large potential difference between two sides of the surface may destroy the low-energy effective approximation for the model's Hamiltonian. The low-energy effective Hamiltonian for the surface states of a 3D TI in the presence of an electrostatic potential is

$$H = \hbar v(\sigma_x k_y - \sigma_y k_x) + V(x), \tag{1}$$

where σ_x and σ_y are the Pauli spin matrices, v the Fermi velocity, and $V(x)$ the electrostatic potential. In units of $\hbar = 1$, the energy spectrum for $V(x) = 0$ is $E = svk$, where $s = \pm 1$. This low-energy effective Hamiltonian is accurate enough for Bi_2Se_3, whose Fermi surface is nearly isotropic, to study the scattering properties of electron states. But for Bi_2Te_3 with a strongly warped surface band, this model is suitable only for the situations where the energy is near the Dirac point.

Firstly, we consider a one-dimensional (1D) square-well potential $V(x) = V_0[\theta(x) - \theta(x-d)]$ on the surface of a TI, where $\theta(x)$ is a step function and d the width of the potential well. With momentum conservation in the y direction, we can express the eigenfunction for Hamiltonian (1) as $\Psi(x,y) = \psi(x)\,\mathrm{e}^{\mathrm{i}k_y y}$, with $\psi(x) = [\phi_1(x), \phi_2(x)]^{\mathrm{T}}$. By substituting the wave function into the eigenequation corresponding to Hamiltonian (1), we obtain

$$\begin{aligned} &\phi_1''(x) + \left[\frac{(V_0 - E)^2}{v^2} - k_y^2\right]\phi_1 = 0, \\ &\phi_2(x) = \frac{v\phi_1' - vk_y\phi_1}{V_0 - E} \end{aligned} \tag{2}$$

for $0 \le x \le d$. In the limitation of $|V_0| \gg E$, we can take the following general form for the wave function

$$\begin{aligned} \psi(x) \;=\; & A\sin\left(\frac{|V_0|}{v}x\right) + B\cos\left(\frac{|V_0|}{v}x\right) \\ & \times \frac{|V_0|}{V_0}\left[A\cos\left(\frac{|V_0|}{v}x\right) - B\sin\left(\frac{|V_0|}{v}x\right)\right], \end{aligned} \tag{3}$$

where A and B are constants. Obviously,

$$\psi(0) = \left[B, \frac{|V_0|}{V_0}A\right]^{\mathrm{T}}$$

according to Eq. (3), hence, the wave function can be rewritten as $\psi(x) = \mathrm{e}^{\mathrm{i}\sigma_y V_0 x/v}\psi(0)$.

To get a δ-function potential located at $x = 0$, let us take the limit of $V_0 \to \infty$ and $d \to 0$, while keeping $V_0 d/v = \alpha$ (constant). Therefore, we have $\psi(d \to 0^+) = \mathrm{e}^{\mathrm{i}\sigma_y\alpha}\psi(0)$; that is,

$$\psi(x \to 0^+) = \mathrm{e}^{\mathrm{i}\sigma_y\alpha}\psi(x \to 0^-). \tag{4}$$

Actually, this boundary condition means that the direction of spin polarization turns an angle of 2α in an anti-clockwise direction in the x–z plane, when tunneling through the step edge. For $\alpha < 0$, it is an angle of $|2\alpha|$ in the clockwise direction.

Next, we consider the effect of the step edge on the surface of a TI in the framework of scattering theory. First, one can write down the following expressions of the wave function for the scattering states with incident momentum $k = (k_x, k_y)$ and the electron group velocity along the x axis $v_x > 0$

$$\psi_{\mathrm{S}}(x < 0) \;=\; \frac{1}{\sqrt{2}}\begin{pmatrix} 1 \\ -\mathrm{i}s\,\mathrm{e}^{\mathrm{i}\theta} \end{pmatrix}\mathrm{e}^{\mathrm{i}k_x x} + r\frac{1}{\sqrt{2}}\begin{pmatrix} 1 \\ \mathrm{i}s\,\mathrm{e}^{-\mathrm{i}\theta} \end{pmatrix}\mathrm{e}^{-\mathrm{i}k_x x},$$

$$\psi_{\rm S}(x>0) = t\frac{1}{\sqrt{2}}\begin{pmatrix}1\\ -{\rm i}s{\rm e}^{{\rm i}\theta}\end{pmatrix}{\rm e}^{{\rm i}k_x x}, \tag{5}$$

where $s=\mathrm{sgn}(E)$, $\theta=\arctan(k_y/k_x)$ is the incident angle, r and t are the reflection and transmission amplitudes, respectively, for the scattering process. Because $v_x(s,\boldsymbol{k})=(\partial E/\partial k_x)_{k_y}=v^2k_x/E$, hence, $v_x>0$ needs $sk_x>0$. Therefore, we can obtain r and t from Eq. (5) with the help of boundary condition (4)

$$\begin{aligned} r &= -\frac{{\rm e}^{{\rm i}\theta}\sin\theta\sin\alpha}{s\cos\alpha\cos\theta+{\rm i}\sin\alpha},\\ t &= \frac{s\cos\theta}{s\cos\alpha\cos\theta+{\rm i}\sin\alpha}. \end{aligned} \tag{6}$$

Consequently, the tunneling probability is obtained by further calculation through $T=|t|^2$ for the scattering process.

Meanwhile, there are possibly exit bound states[33,34] along the step line edge and they decay exponentially as $x\to\pm\infty$. The general form of its wave function can be written as

$$\begin{aligned} \psi_{\rm B}(x<0) &= C{\rm e}^{\kappa x}\begin{pmatrix}E\\ v(k_y-\kappa)\end{pmatrix},\\ \psi_{\rm B}(x>0) &= C{\rm e}^{-\kappa x}\begin{pmatrix}E\\ v(k_y+\kappa)\end{pmatrix}, \end{aligned} \tag{7}$$

where $\kappa^2=k_y^2-E^2/v^2$, C is a constant to be determined. By matching the wave functions (5) at the line edge with boundary condition (4), we obtain the energy dispersion for bound states: $-E\tan\alpha=v\kappa$, hence, $E=\pm vk_y\cos\alpha$. Because the value of $E\tan\alpha$ must be negative, the sign of E is determined for a given α. This is a physical realization of the Tomonaga model, which is well described in Ref. [45], but here we derive it in a different approach. Therefore, the final form of normalized wave function for the bound states is obtained

$$\begin{aligned} \psi_{\rm B}(x<0) &= \sqrt{\frac{-sk_y\sin\alpha}{2(1+s\sin\alpha)}}{\rm e}^{-sk_yx\sin\alpha}\begin{pmatrix}\cos\alpha\\ s+\sin\alpha\end{pmatrix},\\ \psi_{\rm B}(x>0) &= \sqrt{\frac{sk_y\sin\alpha}{2(1-s\sin\alpha)}}{\rm e}^{sk_yx\sin\alpha}\begin{pmatrix}\cos\alpha\\ s-\sin\alpha\end{pmatrix}. \end{aligned} \tag{8}$$

Finally, we can calculate the LDOS near the step edge by summing over all possible independent states. For $E\tan\alpha>0$, there are no bound states. So that the LDOS only has a contribution to the scattering states as

$$\rho_{\rm S}(x,E)=\sum_{s,k_x,k_y}|\psi_{\rm S}|^2\,\delta(E-E_{\rm S}). \tag{9}$$

For $E\tan\alpha<0$, in contrast, the bound states make an important contribution to the LDOS in the vicinity of the step edge as

$$\begin{aligned} \rho_{\rm B}(x<0,E) &= \sum_{s,k_y}|\psi_{\rm B}|^2\,\delta(E-E_{\rm B})\\ &= -\frac{E}{2\pi v^2}\frac{\tan\alpha}{\cos\alpha}{\rm e}^{-2Ex\tan\alpha/v}. \end{aligned} \tag{10}$$

Therefore, when we study the LDOS near a step line edge on the surface of a 3D TI, the contributions of both scattering and bound states should be taken into account; that is, the total LDOS is

$$\rho(x,E)=\rho_{\rm S}(x,E)+\rho_{\rm B}(x,E). \tag{11}$$

In the rest of this section, we give a few numerical examples of the spatial distribution of spin polarization and LDOS for the system of a step line edge on the surface of a 3D TI. We note that the numerical calculation here do not depend on the detailed material parameters.

In Fig. 1, we plot the spatial distribution of spin polarization for a scattering state with incident angle $\theta=\pi/6$ and δ-function potential strength $\alpha=\pi/3$, where the (red) dashed line for $\langle\sigma_x\rangle$, (blue) dotted line for $\langle\sigma_y\rangle$, (green) dash–dotted line for $\langle\sigma_z\rangle$, and (black) solid line for $\langle\sigma_{xz}\rangle$. As is shown in the figure, the electron spin polarization $\langle\sigma_x\rangle$ and $\langle\sigma_z\rangle$ components oscillate periodically along the x axis in the region $x<0$ owing to the interference of incident and reflected waves. In the region $x>0$, on the contrary, the spin is locked in the surface plane [$\langle\sigma_z\rangle=0$, see the (green) dash–dotted line] because there is only a transmitted plane wave. We note that the components of spin polarization $\langle\sigma_x\rangle$ and $\langle\sigma_z\rangle$ are not continuous at $x=0$, while $\langle\sigma_y\rangle$ and the spin polarization on the x–z plane $\langle\sigma_{xz}\rangle$ are continuous. This indicates that the direction of spin polarization changed suddenly at the step edge. As mentioned above, the direction of the spin polarization turns an angle of 2α in anti-clockwise direction in the x–z plane when tunneling through the δ-function potential. Therefore, in the rest of this paper, we limit the range $-\pi/2\le\alpha\le\pi/2$, unless otherwise stated, because the physics for α and $\alpha+\pi$ are the same.

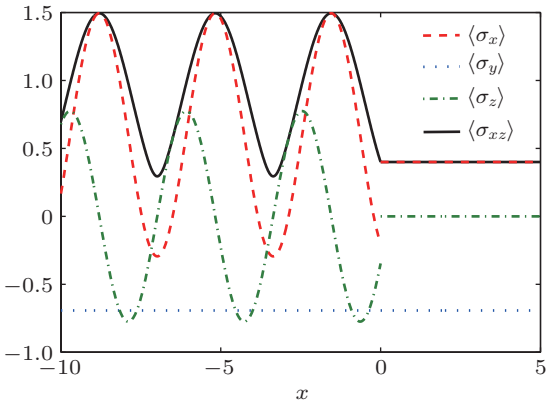


Fig. 1. (color online) The spatial distribution of spin polarization for a surface state scattered from a step edge on the surface of a 3D TI, where the incident angle $\theta=\pi/6$ and the δ-function potential strength $\alpha=\pi/3$.

In order to further explain the electron spin rotation at the step line edge, figure 2(a) presents the transmission probability T versus potential strength parameter α and incident angle θ. As we can see from the figure, T oscillates periodically with

α in a period of π, which ensures our above conclusion. Obviously, T is always 100% (perfect transmission) in the case of low incident angles because the backscattering of surface states by nonmagnetic impurities is completely suppressed.[24] On the other hand, perfect transmission is always achieved for any incident angle θ when potential strength parameter $\alpha = n\pi$ (where n is an integer), which is similar to the resonant tunneling in graphene quantum wells.[46,47] This happens because the step line edge has no effect of obstruction to electrons due to the unchanged spin direction.

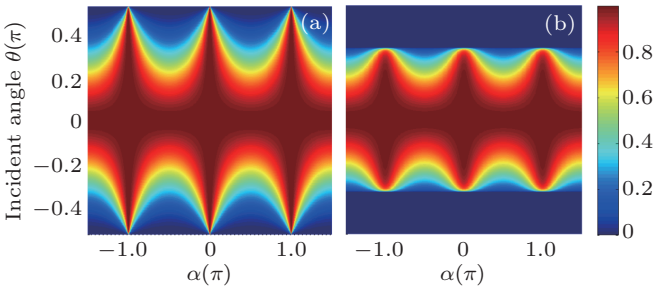


Fig. 2. (color online) Transmission probability T versus δ-function potential strength parameter α and incident angle θ, where (a) for a step line edge on a single 3D TI surface, and (b) for a line edge where two surfaces meet from surface 2 to surface 1, with $v_2/v_1 = 5/6$.

Next, figure 3 shows the calculated LDOS in one side of a step line edge with δ-function potential strength parameters $\alpha = \pm\pi/4$ on a single 3D TI surface, where the (black) solid curve in the main/inset figure for $\rho_{S/B}(x,E)$ stemming from pure scattering/bound states, the (red) dashed curve for the total $\rho(x,E)$ contributed by both scattering and bound states, and the (blue) dotted curves are plotted from the expression $1\pm[1/(2\pi kx)]^{3/2}$ for their envelope. It is clearly seen that the LDOS decays monotonically $x^{-3/2}$ away from the step defect, which is in agreement with recent STM experimental observation[35] and theoretical predictions[29–32] on Bi_2Se_3. This faster decay, in comparison with the $x^{-1/2}$ decay seen in the conventional 2DEG,[41] implies the nature of Dirac electrons on 3D TIs. Importantly, the (black) solid line in the inset figure for the LDOS stemming from bound states shows a very sharp peak, that is, the LDOS is very large near the step edge, but exponentially decays rapidly away from it with the decay length $v/2E\,|\tan\alpha|$. Consequently, this leads to a very strong total LDOS near the step edge, as shown by the (red) dashed line. Far away from the step edge, however, the bound states do not modify the exponential behavior of the LDOS oscillations. Moreover, it is worth mentioning that, when $\alpha = n\pi$ (where n is an integer), the LDOS oscillations will disappear because that there is no spin rotation at the step, as indicated in Fig. 1 and Fig. 2(a).

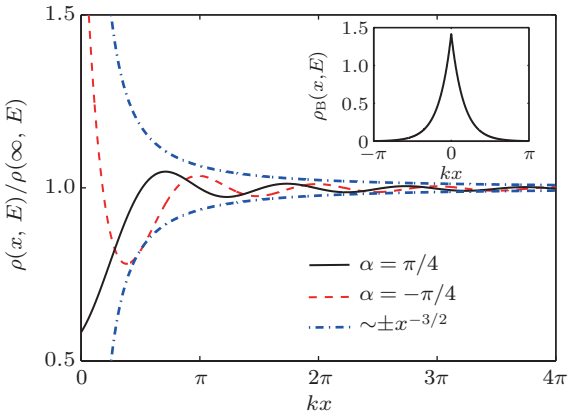


Fig. 3. (color online) LDOS above the Dirac point near a step line edge on 3D TI surface with $\alpha = \pm\pi/4$, where the (black) solid curve for the LDOS stemming from pure scattering states, the (red) dashed curve for the LDOS stemming from both scattering and bound states. The (blue) dotted curves plotted from expression $1\pm[1/(2\pi kx)]^{3/2}$ are their envelope decaying as $x^{-3/2}$, where k is the wave vector at energy E and $\rho(\infty,E) = |E|/2\pi v^2$ the LDOS in the absence of the step edge. The inset shows the LDOS stemming from pure bound states.

3. A line edge where two surfaces meet for a finite 3D TI

In this section, we study the surface states scattering off a line edge where the front and side surfaces meet with different velocities v_1 and v_2 for a finite strong 3D TI. Without losing the generality, we definitely presume that $v_1 > v_2$. Here we are only interested in the LDOS oscillations away from the edge, which is easily detected by an STM tip. Hence, we ignore the bound states that make no contribution to the decaying exponent of the LDOS at long distance, as discussed in Section 2.

The low-energy physics of the two surfaces can be well described by the effective Hamiltonians

$$H_1 = v_1(\sigma_x k_y - \sigma_y k_x), \quad H_2 = v_2(\sigma_x k_y - \sigma_y k_x). \tag{12}$$

The wave functions are given as follows for left and right incident waves with wave vectors $\boldsymbol{k} = (k_x, k_y)$ and $\boldsymbol{k}' = (-k'_x, k_y)$, respectively,

$$\begin{aligned}
\psi_{\rm L}(x<0) &= \frac{1}{\sqrt{2}}\begin{pmatrix} 1 \\ \dfrac{v_1(k_y - {\rm i}k_x)}{E} \end{pmatrix} {\rm e}^{{\rm i}k_x x} \\
&\quad + r\frac{1}{\sqrt{2}}\begin{pmatrix} 1 \\ \dfrac{v_1(k_y + {\rm i}k_x)}{E} \end{pmatrix} {\rm e}^{-{\rm i}k_x x}, \\
\psi_{\rm L}(x>0) &= t\frac{1}{\sqrt{2}}\begin{pmatrix} 1 \\ \dfrac{v_2(k_y - {\rm i}k'_x)}{E} \end{pmatrix} {\rm e}^{{\rm i}k'_x x}, \\
\psi_{\rm R}(x>0) &= \frac{1}{\sqrt{2}}\begin{pmatrix} 1 \\ \dfrac{v_2(k_y + {\rm i}k'_x)}{E} \end{pmatrix} {\rm e}^{-{\rm i}k'_x x} \\
&\quad + r'\frac{1}{\sqrt{2}}\begin{pmatrix} 1 \\ \dfrac{v_2(k_y - {\rm i}k'_x)}{E} \end{pmatrix} {\rm e}^{{\rm i}k'_x x}, \\
\psi_{\rm R}(x<0) &= t'\frac{1}{\sqrt{2}}\begin{pmatrix} 1 \\ \dfrac{v_1(k_y + {\rm i}k_x)}{E} \end{pmatrix} {\rm e}^{-{\rm i}k_x x}.
\end{aligned} \tag{13}$$

with $E = sv_1\sqrt{k_x^2+k_y^2} = sv_2\sqrt{k_x'^2+k_y^2}$.

Similar to that used in Section 2, we model the line edge as a δ-function scattering potential which located at $x = 0$, with different Fermi velocities in two sides, $x < 0$ and $x > 0$.[46] Considering the current conservation, we can get the boundary condition at the line edge as

$$\psi(x \to 0^+) = \sqrt{v_1/v_2}\, e^{i\sigma^y \alpha}\psi(x \to 0^-),$$

with which one can obtain the reflection and transmission amplitudes of the scattered waves incident from both sides, respectively. The expressions are

$$\begin{aligned}
r &= e^{i\theta}\frac{s\cos\alpha\sin\left(\frac{\theta-\theta'}{2}\right)+i\sin\alpha\sin\left(\frac{\theta+\theta'}{2}\right)}{\sin\alpha\cos\left(\frac{\theta-\theta'}{2}\right)-is\cos\alpha\cos\left(\frac{\theta+\theta'}{2}\right)},\\
t &= -\sqrt{\frac{v_1}{v_2}}\frac{is\cos\theta\exp\left[i\left(\frac{\theta-\theta'}{2}\right)\right]}{\sin\alpha\cos\left(\frac{\theta-\theta'}{2}\right)-is\cos\alpha\cos\left(\frac{\theta+\theta'}{2}\right)},\\
r' &= -e^{-i\theta'}\frac{s\cos\alpha\sin\left(\frac{\theta'-\theta}{2}\right)+i\sin\alpha\sin\left(\frac{\theta'+\theta}{2}\right)}{\sin\alpha\cos\left(\frac{\theta'-\theta}{2}\right)-is\cos\alpha\cos\left(\frac{\theta'+\theta}{2}\right)},\\
t' &= -\sqrt{\frac{v_2}{v_1}}\frac{is\cos\theta'\exp\left[i\left(\frac{\theta'-\theta}{2}\right)\right]}{\sin\alpha\cos\left(\frac{\theta'-\theta}{2}\right)-is\cos\alpha\cos\left(\frac{\theta'+\theta}{2}\right)},
\end{aligned} \tag{14}$$

where $s = \mathrm{sgn}(E)$, $\theta = \tan^{-1}(k_y/k_x)$, and $\theta' = \tan^{-1}(k_y/k_x')$. The energy conservation requires that $v_1(k_x^2+k_y^2)^{1/2} = v_2(k_x'^2+k_y^2)^{1/2}$. Therefore, we can obtain a relation $\sin\theta/v_1 = \sin\theta'/v_2$, which is similar to the Snell's law in optics. We can also obtain the transmission probability as $T(T') = 1 - |r(r')|^2$, where $T(T')$ represents the transmission probability from surface 2(1) to surface 1(2). Note that our expressions (14) are consistent with those in Ref. [44], but different notations are used here.

Figure 2(b) presents the transmission probability T as a function of δ-function potential strength parameter α and incident angle θ, incident from surface 2 to surface 1 with $v_2/v_1 = 5/6$. Similar to the case of a step line edge, T also oscillates periodically with α in a period of π, and shows perfect transmission with low incident angles. Moreover, the total reflection occurs similarly to optics in the large incident angle case. Here, we have omitted the transmission probability T' due to its similarity with Fig. 2(a).

The LDOS observed by STM experiments should include the contributions of both left and right incident waves. So we construct the new energy eigenstates as follows:[27]

$$\psi_{\mathrm{L}}^{\mathrm{new}} = \frac{|s,k_x,k_y\rangle_{\mathrm{L}} + r(\boldsymbol{k})\,|s,-k_x,k_y\rangle_{\mathrm{L}} + t(\boldsymbol{k})\,|s,k_x',k_y\rangle_{\mathrm{R}}}{\sqrt{2}},$$

$$\psi_{\mathrm{R}}^{\mathrm{new}} = \frac{|s,-k_x',k_y\rangle_{\mathrm{R}} + r'(\boldsymbol{k}')\,|s,k_x',k_y\rangle_{\mathrm{R}} + t'(\boldsymbol{k}')\,|s,-k_x,k_y\rangle_{\mathrm{L}}}{\sqrt{2}}. \tag{15}$$

for the left and right incident waves as well as their outgoing ones, respectively, with $sk_x, sk_x' > 0$. On the other hand, there will be states of total reflection $\psi_{\mathrm{R}}^{\mathrm{tr}}$ on surface 2 as

$$\psi_{\mathrm{R}}^{\mathrm{tr}} = \frac{|s,-k_x',k_y\rangle_{\mathrm{R}} + r'(\boldsymbol{k}')\,|s,k_x',k_y\rangle_{\mathrm{R}}}{\sqrt{2}}, \tag{16}$$

where $r'(\boldsymbol{k}') = e^{i\varphi(\alpha,\theta')}$ with the angle for total reflection $\theta' > \theta_{\mathrm{c}} = \sin^{-1}(v_2/v_1)$. Including both the contributions of scattering states and the states of total reflection, the total LDOS is obtained as

$$\begin{aligned}
\rho(x,E) = &\sum_{\substack{sk_x,sk_x'>0,\ k_y,\\ \theta'<\theta_c}} \left(|\psi_{\mathrm{L}}^{\mathrm{new}}|^2 + |\psi_{\mathrm{R}}^{\mathrm{new}}|^2\right)\delta(E-E_{\mathrm{S}})\\
&+ \sum_{\substack{sk_x,sk_x'>0,\ k_y,\\ \theta'>\theta_c}} |\psi_{\mathrm{R}}^{\mathrm{tr}}|^2\,\delta(E-E_{\mathrm{S}}).
\end{aligned} \tag{17}$$

In Fig. 4, we present the LDOS with $\alpha = \pi/4$ and two ratios of the Fermi velocities v_1/v_2 in certain energy, where the (black) solid line stands for $v_1/v_2 = 1.01$, the (red) dashed line stands for $v_1/v_2 = 1.1$, and the (blue) and (green) dash–dotted lines stand for their decaying envelope, respectively. Obviously, it is seen that a line edge on the surface of topological insulators induces standing waves in LDOS, which is discontinuous at $x = 0$ with quite different oscillation feature in the two sides (asymmetry). The wave vector of LDOS oscillations is sensitive to the ratio of v_1/v_2 and is no longer equal to the diameter of CEC of surface band, which is unlike the situation in the step line edge on single 3D TI surface in surface 2 (with the smaller Fermi velocity). It also shows a slower decay $x^{-1/2}$ far from the line edge, even though it does not fit the decay curve in the vicinity, which is in contrast with the $x^{-3/2}$ decay in the case of step edge. However, the LDOS feature in surface 1 (with the greater Fermi velocity) is nearly the same as that in the step edge case. These distinct behaviors of LDOS oscillation in the two sides are believed to partially be the result of the total reflection. Actually, we also obtained some plots for the velocity ratio v_1/v_2 far away from 1, such as 2, 2.1, and so on, which is not presented here because of the limitation of space. The new decaying behavior $x^{-1/2}$ did not change with the velocity ratio v_1/v_2. It is interesting that if v_1 and v_2 are not quite the same, such as $v_1/v_2 = 1.01$, the new decaying behavior $x^{-1/2}$ just appears. This indicates that the new decaying behavior appears with the total reflection's appearance. We also obtained a plot for $\alpha = \pi/8$, which is still not presented here because of the limitations of space. The result shows that the LDOS behavior is not sensitively dependent on the value of α; that is, it is model-independent.

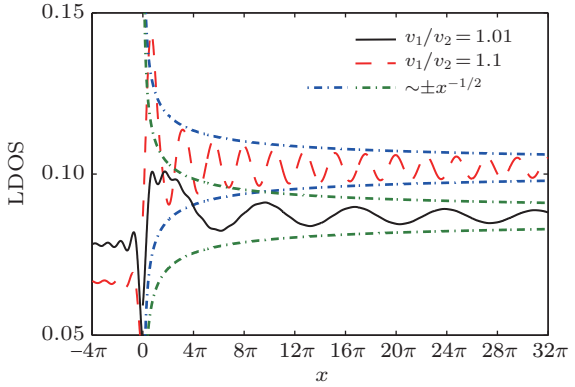


Fig. 4. (color online) LDOS as a function of distance from the line edge along the x axis with different velocity ratios, where the (black) solid line for $v_1/v_2 = 1.01$, the (red) dashed line for $v_1/v_2 = 1.1$, (v_1 is for $x < 0$, v_2 for $x > 0$), and the dash–dotted curves are their envelopes decaying as $x^{-1/2}$ (the blue lines are from $0.102 \pm \sqrt{1/600\pi x}$, and the green ones are from $0.087 \pm \sqrt{1/600\pi x}$).

4. Summary

In summary, by using a δ-function potential to model an atomic step line edge on the surface of a single 3D TI and a line edge between two surfaces of a 3D TI with different Fermi velocities, we have studied the decaying behavior of LDOS oscillations near and away from the edges, respectively. For the step line edge on single surface, the bound states existed along the step edge significantly contribute to the LDOS near the edge, but do not modify the exponential behavior of the LDOS oscillations away from it. Importantly, this effect may explain the anomalous behavior of LDOS oscillation near the step observed by recent STM experiments. In addition, the recovered $x^{-3/2}$ power-law decaying behavior for LDOS oscillation away from the step is also understood from the spin rotation for surface states scattering off the step defect with magnitude depending on the strength of the δ-function potential. For a line edge, the electron refraction and total reflection occur at the edge, which is analogous to optics. By ignoring the influence of bound states, we show that the LDOS oscillating decay behavior in the greater Fermi velocity side is similar to that for a step line edge on a single TI surface. However, in the smaller Fermi velocity side away from the edge, the LDOS oscillation shows a decaying behavior as $x^{-1/2}$, and the wavevector of the LDOS oscillations is no longer equal to the diameter of the CEC of surface band but is sensitive to the ratio of the two Fermi velocities. We hope that these effects for general TI materials may be verified by STM with high precision.

References

[1] Qi X L and Zhang S C 2010 *Phys. Today* **63** 33
[2] Moore J E 2010 *Nature* **464** 194
[3] Fu L, Kane C L and Mele E J 2007 *Phys. Rev. Lett.* **98** 106803
[4] Moore J E and Balents L 2007 *Phys. Rev. B* **75** 121306
[5] Bernevig B A, Hughes T L and Zhang S C 2006 *Science* **314** 1757
[6] Zhang H, Liu C X, Qi X L, Dai X, Fang Z and Zhang S C 2009 *Nat. Phys.* **5** 438
[7] König M, Wiedmann S, Brüne C, Roth A, Buhmann H, Molenkamp L W, Qi X L and Zhang S C 2007 *Science* **318** 766
[8] Xia Y, Qian D, Hsieh D, Wray L, Pal A, Lin H, Bansil A, Grauer D, Hor Y S, Cava R J and Hasan M Z 2009 *Nat. Phys.* **5** 398
[9] Chen Y L, Analytis J G, Chu J H, Liu Z K, Mo S K, Qi X L, Zhang H J, Lu D H, Dai X, Fang Z, Zhang S C, Fisher I R, Hussain Z and Shen Z X 2009 *Science* **325** 178
[10] Hsieh D, Xia Y, Wray L, Qian D, Pal A, Dil J H, Osterwalder J, Meier F, Bihlmayer G, Kane C L, Hor Y S, Cava R J and Hasan M Z 2009 *Science* **323** 919
[11] Roushan P, Seo J, Parker C V, Hor Y S, Hsieh D, Qian D, Richardella A, Hasan M Z, Cava R J and Yazdani A 2009 *Nature* **460** 1106
[12] Hasan M Z and Kane C L 2010 *Rev. Mod. Phys.* **82** 3045
[13] Qi X L and Zhang S C 2011 *Rev. Mod. Phys.* **83** 1057
[14] Fu L and Kane C L 2008 *Phys. Rev. Lett.* **100** 096407
[15] Qi X L, Hughes T L, Raghu S and Zhang S C 2009 *Phys. Rev. Lett.* **102** 187001
[16] Qi X L, Li R, Zang J and Zhang S C 2009 *Science* **323** 1184
[17] Sakamoto Y, Hirahara T, Miyazaki H, Kimura S and Hasegawa S 2010 *Phys. Rev. B* **81** 165432
[18] Zyuzin A A, Hook M D and Burkov A A 2011 *Phys. Rev. B* **83** 245428
[19] Brahlek M, Bansal N, Koirala N, Xu S Y, Neupane M, Liu C, Hasan M Z and Oh S 2012 *Phys. Rev. Lett.* **109** 186403
[20] He H, Li B, Liu H, Guo X, Wang Z, Xie M and Wang J 2012 *Appl. Phys. Lett.* **100** 032105
[21] Wang J, DaSilva A M, Chang C Z, He K, Jain J K, Samarth N, Ma X C, Xue Q K and Chan M H W 2011 *Phys. Rev. B* **83** 245438
[22] Liu Y M, Shao H H, Zhou X Y and Zhou G H 2013 *Chin. Phys. B* **22** 077310
[23] Shao H H, Zhou X Y, Li Y, Liu G H and Zhou G H 2011 *Appl. Phys. Lett.* **99** 153104
[24] Zhang T, Cheng P, Chen X, Jia J F, Ma X, He K, Wang L, Zhang H, Dai X, Fang Z, Xie X C and Xue Q K 2009 *Phys. Rev. Lett.* **103** 266803
[25] Lee W C, Wu C, Arovas D P and Zhang S C 2009 *Phys. Rev. B* **80** 245439
[26] Guo H M and Franz M 2010 *Phys. Rev. B* **81** 041102(R)
[27] Fu Z G, Zhang P, Wang Z and Li S S 2011 *Phys. Rev. B* **84** 235438
[28] Wang J and Zhu B F 2013 *Chin. Phys. B* **22** 067301
[29] Biswas R R and Balatsky A V 2011 *Phys. Rev. B* **83** 075439
[30] Biswas R R and Balatsky A V 2011 arXiv: 1005.4780
[31] Zhou X, Fang C, Tsai W F and Hu J P 2009 *Phys. Rev. B* **80** 245317
[32] Wang Q H, Wang D and Zhang F C 2010 *Phys. Rev. B* **81** 035104
[33] Alpichshev Z, Analytis J G, Chu J H, Fisher I R, Chen Y L, Shen Z X, Fang A and Kapitulnik A 2010 *Phys. Rev. Lett.* **104** 016401
[34] Alpichshev Z, Analytis J G, Chu J H, Fisher I R and Kapitulnik A 2011 *Phys. Rev. B* **84** 041104(R)
[35] Wang J, Li W, Cheng P, Song C, Zhang T, Deng P, Chen X, Ma X, He K, Jia J F, Xue Q K and Zhu B F 2011 *Phys. Rev. B* **84** 235447
[36] Zhang D and Ting C S 2012 *Phys. Rev. B* **85** 115434
[37] An J and Ting C S 2012 *Phys. Rev. B* **86** 165313
[38] Deb O, Soori A and Sen D 2014 arXiv: 1401.1027
[39] Rakyta P, Pályi A and Cserti J 2012 *Phys. Rev. B* **86** 085456
[40] Herath T M, Hewageegana P and Apalkov V 2013 *Phys. Rev. B* **87** 075318
[41] Crommie M F, Lutz C P and Eigler D M 1993 *Nature* **363** 524
[42] Moon C Y, Han J, Lee H and Choi H J 2011 *Phys. Rev. B* **84** 195425
[43] Zhang Y Y, Wang X R and Xie X C 2012 *J. Phys.: Condens. Matter* **24** 015004
[44] Takahashi R and Murakami S 2011 *Phys. Rev. Lett.* **107** 166805
[45] Yokoyama T, Balatsky A V and Nagaosa N 2010 *Phys. Rev. Lett.* **104** 246806
[46] Sen D and Deb O 2012 *Phys. Rev. B* **85** 245402
[47] Pereira J M, Mlinar J V, Peeters F M and Vasilopoulos P 2006 *Phys. Rev. B* **74** 045424